Non-Gaussian polymers described by alpha-stable chain statistics: Model, effective interactions in binary mixtures, and application to on-surface separation

M. Majka* and P. F. Góra

Marian Smoluchowski Institute of Physics, Jagiellonian University, ul. prof. Stanisława Łojasiewicza 11, 30-348 Kraków, Poland

(Received 22 January 2015; published 13 May 2015)

The Gaussian chain model is the classical description of a polymeric chain, which provides analytical results regarding end-to-end distance, the distribution of segments around the mass center of a chain, coarse-grained interactions between two chains and effective interactions in binary mixtures. This hierarchy of results can be calculated thanks to the α stability of the Gaussian distribution. In this paper we show that it is possible to generalize the model of Gaussian chain to the entire class of α-stable distributions, obtaining the analogous hierarchy of results expressed by the analytical closed-form formulas in the Fourier space. This allows us to establish the α-stable chain model. We begin with reviewing the applications of Levy flights in the context of polymer sciences, which include: chains described by the heavy-tailed distributions of persistence length; polymers adsorbed to the surface; and the chains driven by a noise with power-law spatial correlations. Further, we derive the distribution of segments around the mass center of the α-stable chain and construct the coarse-grained interaction potential between two chains. These results are employed to discuss the model of binary mixture consisting of the α-stable chains. In what follows, we establish the spinodal decomposition condition generalized to the mixtures of the α-stable polymers. This condition is further applied to compare the on-surface phase separation of adsorbed polymers (which are known to be described with heavy-tailed statistics) with the phase separation condition in the bulk. Finally, we predict the four different scenarios of simultaneous mixing and demixing in the two- and three-dimensional systems.

DOI: 10.1103/PhysRevE.91.052602 PACS number(s): 36.20.−r, 05.40.Fb, 68.35.Dv, 82.35.Gh

I. INTRODUCTION

While the theory of Flory provides an accurate description of the ideal polymeric chains [1], factors such as complex environment interactions, adsorption, or designed chemical composition can lead to significant deviations from this model. The Flory approach is based on the Gaussian chain model, in which the conformation of a chain is equivalent to the trajectory of a particle undergoing the thermal Brownian motion [1]. In this model the chain is characterized by the Gaussian distribution of the nearest-neighbor distances, a fact that leads to the entire hierarchy of analytical results. In particular, the Gaussian shape propagates to such characteristics as end-to-end distance distribution [1], distribution of segments around the mass center of the chain [2], and the coarse-grained interaction potential between two chains in terms of the distance between their mass centers [3]. Deriving all of these characteristics is possible due to a single fact: the Gaussian distribution is α stable. Since there exists the entire class of α-stable, heavy-tailed distributions [4], this suggests that a natural and equally prolific generalization of the Gaussian chain model can be based on the α-stable distributions. Indeed, in this paper we discuss the α-stable chain model and calculate all of the characteristics analogous to the Gaussian model.

The first goal of this paper is to establish the physical context in which the α-stable distributions are relevant for the polymer sciences. Since the application of α-stable distributions (or Levy walks and Levy flights) in this context is not an entirely new concept, in Sec. II we review the relevant literature. In addition, we provide our own simulations of a model polymeric chain under the spatially correlated noise, which establish another context for our considerations.

The main part of this paper is focused on deriving and analyzing the different aspects of the α-stable chain model. In Sec. III we introduce the model itself. The distribution of nodes around the mass center of a chain is calculated in Appendix. In Sec. IV the coarse-grained model of interaction between two chains is established. All of these results are analytical and closed form in the Fourier space.

Another goal of this paper is to analyze the stability of binary mixtures composed of the α-stable chains. Understanding the behavior of binary mixtures is a vital problem in industry, medicine, wet nanotechnology, and biophysics. Usually, this problem is considered in the framework of spinodal decomposition. In this approach the local extremes of the free-energy functional are identified with respect to the thermodynamical parameters. While the local minima are associated with stable thermodynamic phases, which are insensitive to the fluctuations of parameters, the local maxima indicate the phase transitions. This method was successfully applied to find the decomposition condition in the mixtures of Gaussian particles [5,6], namely, there exists a well defined region of mixing and demixing, dependent on the proportion of gyration radii.

From the microscopic perspective, the stability of solution is governed by effective interactions [7], whose prediction is a classical problem of soft matter physics [8]. In the context of binary mixtures of Gaussian particles, Bolhuis *et al.* found via simulations that the interaction between particles of one species has also a Gaussian profile, but with an addition of a shallow attractive tail [9]. Similar results were predicted half analytically via closure-relations techniques in Refs. [10,11]. On the other hand, a simpler, but entirely analytical method has been recently proposed in Ref. [12] by the authors of

*maciej.majka@uj.edu.pl

 ©2015 American Physical Society

this paper. Therein, we have studied the stability of Gaussian particles mixtures and our results proved similar to the spinodal decomposition analysis [5,6]. Since our methodology from Ref. [12] can be conveniently extended to the particles described with the α-stable profiles, we apply this approach in the current paper. As the main result of Sec. V, we generalize the spinodal decomposition condition for Gaussian particles to the entire class of particles based on the α-stable distributions. We discuss the validity of our methodology in Sec. VI.

Finally, in Sec. VII we employ the results regarding phase separation in binary mixtures to analyze the phase separation of adsorbed polymers versus their behavior in the bulk. As a result we predict the parameters for which the different combinations of simultaneous mixing or demixing on the surface and in the bulk can be achieved.

II. LEVY FLIGHTS IN POLYMER SCIENCES

Except for the Gaussian case, the asymptotic behavior of the α-stable distributions is of the power-law type $\propto 1/r^{\alpha+1}$ [4], where $\alpha \in [0,2]$ is the characteristic exponent of the distribution. A random walk characterized by such a heavy-tailed distribution of steps is known as a Levy flight. It is usually difficult to interpret Levy flights in physical terms, therefore let us discuss three situations justifying such statistics in the context of polymers.

The first scenario can be related to the non-Gaussian distribution of segment persistence lengths. The Gaussian chain model is usually derived from a discrete model, in which all segments have the same persistence length [1]. However, it can be also seen as the model for a chain made of unequal segments, whose persistence lengths follow the Gaussian distribution. This can be further generalized to the α-stable distribution, the idea suggested by Moon and Nakanishi in Ref. [13]. They proposed the Levy walk chain model, based on the formalism of turbulent flows [14] and calculated Flory exponents for this model. While no direct experimental confirmation of this idea is known to the present authors, non-Gaussian persistence length distribution might be the result of the varying chemical composition of a chain. For example, the DNA double strand is characterized by the persistence length much greater than a single base pair [15], but also certain sequences of chemical monomers can assemble into relatively long and stable structures of significant persistence length, such as protein domains [16]. A possible realization of such Levy flights could be the intrinsically disordered proteins, in which second-order structural motifs such as α helices coexist with disordered loops [17,18]. However, it should be mentioned that some numerical experiments on the structure of partially unfolded proteins indicate that Gaussian statistics is rather robust [19].

Another scenario is similar to the problem of a tracer, which mixes one- and three-dimensional diffusion. Such motion has been observed experimentally in DNA-binding proteins [20] and its simulations revealed the heavy-tailed distributions of steps along the polymer in certain configurations [21]. This behavior can be efficiently modeled with Levy flights [22]. In the context of polymers, we consider the adsorption of a chain to the surface. This problem was first analyzed by de Gennes from the scaling perspective in Refs. [23,24].

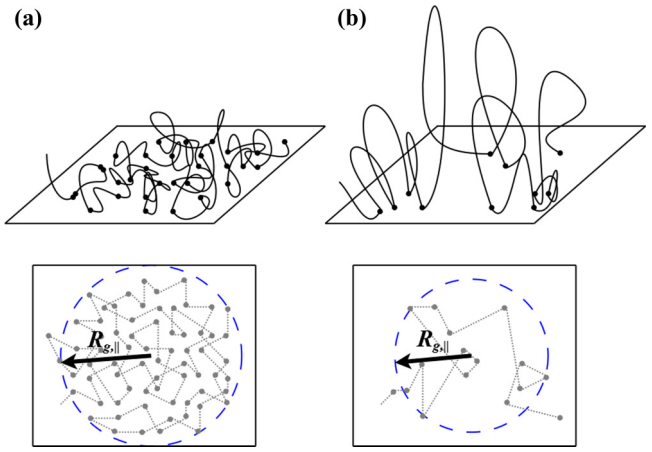

FIG. 1. (Color online) Top: schematic representation of a polymer adsorbed to the surface, dots indicate the adsorbed segments. Bottom: planar trajectories connecting the subsequent adsorbed segments. (a) In the strong adsorption regime freely-diffusing loops are short and subsequent adsorbed nodes are found close to each other. The radius of gyration parallel to the surface scale as $R_{g,||} \propto N^{3/4}$ [25]. (b) In the weak adsorption limit the long, freely diffusing loops are numerous and introduce Levy flights into the planar trajectory. $R_{g,||}$ scales as $\propto N^{3/5}$ [25].

For the intermediate attraction strength, only some fraction of segments is attached to the surface, while the loops that connect those segments diffuse into the bulk. Considering the projection of the chain on the surface, it has been argued by Bouchaud and Daoud [25] that the planar trajectory connecting adsorbed nodes can be modeled as Levy flights, since the subsequent adsorbed segments connected by a loop can be found at abnormally long distances. The schematic representation of a polymer in the strong versus the weak adsorption limit is shown in Fig. 1. Bouchaud and Daoud predict that for an adsorbed polymer its gyration radius parallel to the surface scales as $R_{g,||} \propto N^{3/4}$ for the strong adsorption and $R_{g,||} \propto N^{3/5}$ for the weak adsorption [25]. Within the Flory-type theory for Levy flights discussed in Ref. [25], the latter translates into the characteristic exponent of the distribution $\alpha = 1$ and the former demands $\alpha = 2$. This means that while in the strong adsorption regime the Levy flights and the Gaussian statistics are equivalent, for the weak adsorption limit $R_{g,||}$ should be modeled with power-law distributions.

One final interpretation can be related to the situation in which a polymer experiences a random, though spatially correlated, behavior of surrounding environment. Such conditions occur in the glassy state, in which the correlations are exponential [26–28], or near crystallization, in which case the scale-free behavior results in the power-law correlations [29]. In Ref. [30] we have simulated a two-dimensional model polymeric chain driven by the spatially correlated noise and observed the effect of spontaneous chain unfolding, i.e., a significant number of segments tends to form linearized structures, scattered along the chain. As we have shown in Ref. [31], this effect was mainly due to the short (2–3 segments) structures, but structures up to 50 segments were also observed. Such elongated fragments may act as Levy flights, provided that their distribution is wide enough.

The model from Ref. [30] consisted of a bead-spring chain with a global Lennard-Jones potential assigned to each bead and a second-nearest-neighbor harmonic interaction to induce nonlinear conformations. The system was driven by the noise $\boldsymbol{\xi}$, whose spatial correlation function read:

$$\langle \boldsymbol{\xi}(\mathbf{r})\boldsymbol{\xi}(\mathbf{r}+\Delta\mathbf{r})\rangle \propto \exp(-|\Delta\mathbf{r}|/\lambda). \tag{1}$$

For the purpose of the current paper we have repeated the simulations from Ref. [30], replacing the exponential correlations in the noise with a heavy-tailed function, based on the Cauchy distribution, namely:

$$\langle \boldsymbol{\xi}(\mathbf{r})\boldsymbol{\xi}(\mathbf{r}+\Delta\mathbf{r})\rangle \propto 1/[1+(|\Delta\mathbf{r}|/\lambda)^2]. \tag{2}$$

The data regarding the linearized fragments has been gather in the same fashion as in Ref. [31]. To improve statistics, the single set of parameters was simulated 128 times, otherwise, the details of the simulations remained the same as in Refs. [30] and [31]. In Fig. 2, we include the representative probability distributions S_n of finding the n-segments-long structure in the chain geometry. The data has been gathered from the regime of noise-dominated dynamics. With the growing correlation length λ the distribution S_n gradually develops a linear region in the log-log plot. For $\lambda \geqslant 40$, where relevant, we have fitted S_n for $n > 17$ with a power-law model $S_n = cn^{-(\alpha+1)}$. We obtain α ranging from 1.18 ± 0.39 to 2.44 ± 0.54, with the relative error typically at the level of 20–30 %. The uncertainty intervals for these values of α overlap with the interval $\alpha \in [0,2]$, which is expected for the asymptotic behavior of the α-stable distributions [4]. For comparison, the data have been also fitted with the exponential decay model $S_n = ae^{-n/b}$. While both the linear and exponential fit describe the tail part of S_n similarly well (in both cases $R^2 \simeq 0.8$) and, most probably, even for $\lambda = 50$ the distribution S_n eventually develops the exponential decay for $n \gg 50$, a power-law-like region suggests that in the special conditions of long-range spatial correlations the α-stable distributions might be a more relevant description of the chain statistics than the Gaussian distribution. For comparison we also include in Fig. 2 the data from Ref. [30], which preserve the exponential form in the entire range of parameters.

III. α-STABLE CHAIN MODEL

In the Gaussian chain model, the geometry of a chain is described as a random walk trajectory, in which the distribution of the distances between nearest neighbors is Gaussian, namely [1]:

$$G(|\mathbf{r}_{i+1}-\mathbf{r}_i|) = \left(\frac{2\pi b^2}{D}\right)^{-D/2} \exp\left(-\frac{D(\mathbf{r}_{i+1}-\mathbf{r}_i)^2}{2b^2}\right). \tag{3}$$

Here, D is the dimension of the system, b is usually interpreted as the length of a segment and $\mathbf{r}_i$ is the vector position of ith node. The characteristic function of G reads:

$$\phi_G(k) = \exp\left(-\frac{2b^2}{D}k^2\right). \tag{4}$$

Let us now consider the generalization of $G(|\mathbf{r}_{i+1}-\mathbf{r}_i|)$ to the α-stable distribution $P(|\mathbf{r}_{i+1}-\mathbf{r}_i|)$. The multivariate α-stable distributions are defined in terms of their characteristic functions, which can be written in the following parametrization [4]:

$$\phi(\mathbf{k}) = \begin{cases} \exp\left(-\int_{S_D} |\mathbf{k}\cdot\mathbf{s}|^\alpha \left(1 - i\,\mathrm{sgn}(\mathbf{k}\cdot\mathbf{s})\tan\frac{\pi\alpha}{2}\right)\Gamma(d\mathbf{s}) + i\mathbf{k}\cdot\boldsymbol{\mu}\right) & \text{for} \quad \alpha \neq 1 \\ \exp\left(-\int_{S_D} |\mathbf{k}\cdot\mathbf{s}| \left(1 + i\,\mathrm{sgn}(\mathbf{k}\cdot\mathbf{s})\frac{2\ln\mathbf{k}\cdot\mathbf{s}}{\pi}\right)\Gamma(d\mathbf{s}) + i\mathbf{k}\cdot\boldsymbol{\mu}\right) & \text{for} \quad \alpha = 1. \end{cases} \tag{5}$$

In the above definition $\Gamma(d\mathbf{s})$ stands for the spectral measure defined on the D-dimensional unit sphere S_D, $\mathbf{k}\cdot\mathbf{s}$ denotes the scalar product, and $\boldsymbol{\mu}$ is the vector of mean values. Since we are interested in the spherically symmetric distributions, we choose the uniform spectral measure $\Gamma(d\mathbf{s}) = \text{const.}$ [32]. Under such choice, and assuming $\boldsymbol{\mu} = 0$, the general parametrization can be simplified to the following form:

$$\phi(k) = \exp\left(-ck^\alpha\right), \tag{6}$$

where $k = |\mathbf{k}|$ and c is a constant. Eq. (4) is a special case of $\phi(k)$, and our choice of c should agree with $\phi_G(k)$ for $\alpha = 2$. Therefore, we postulate that c reads:

$$c = \frac{2b^\alpha}{D} \tag{7}$$

and, finally, the nearest-neighbor spatial distribution in the α-stable chain model reads:

$$P(|\mathbf{r}_{i+1}-\mathbf{r}_i|) = \frac{1}{(2\pi)^D}\int d\mathbf{k}\exp\left(i\mathbf{k}\cdot(\mathbf{r}_{i+1}-\mathbf{r}_i) - \frac{2}{D}b^\alpha k^\alpha\right). \tag{8}$$

Having established the nearest-neighbor spatial distribution $P(|\mathbf{r}_{i+1}-\mathbf{r}_i|)$, we can calculate such distribution for any pair of segments, namely:

$$\begin{aligned} P(|\mathbf{r}_i - \mathbf{r}_j|) &= \int d\mathbf{r}_{i+1}\ldots\int d\mathbf{r}_{j-1}\prod_{n=i+1}^{j} P(|\mathbf{r}_n - \mathbf{r}_{n-1}|) \\ &= \frac{1}{(2\pi)^D}\int d\mathbf{k}\exp\left(i\mathbf{k}\cdot(\mathbf{r}_i-\mathbf{r}_j) - \frac{2}{D}|i-j|b^\alpha k^\alpha\right), \end{aligned} \tag{9}$$

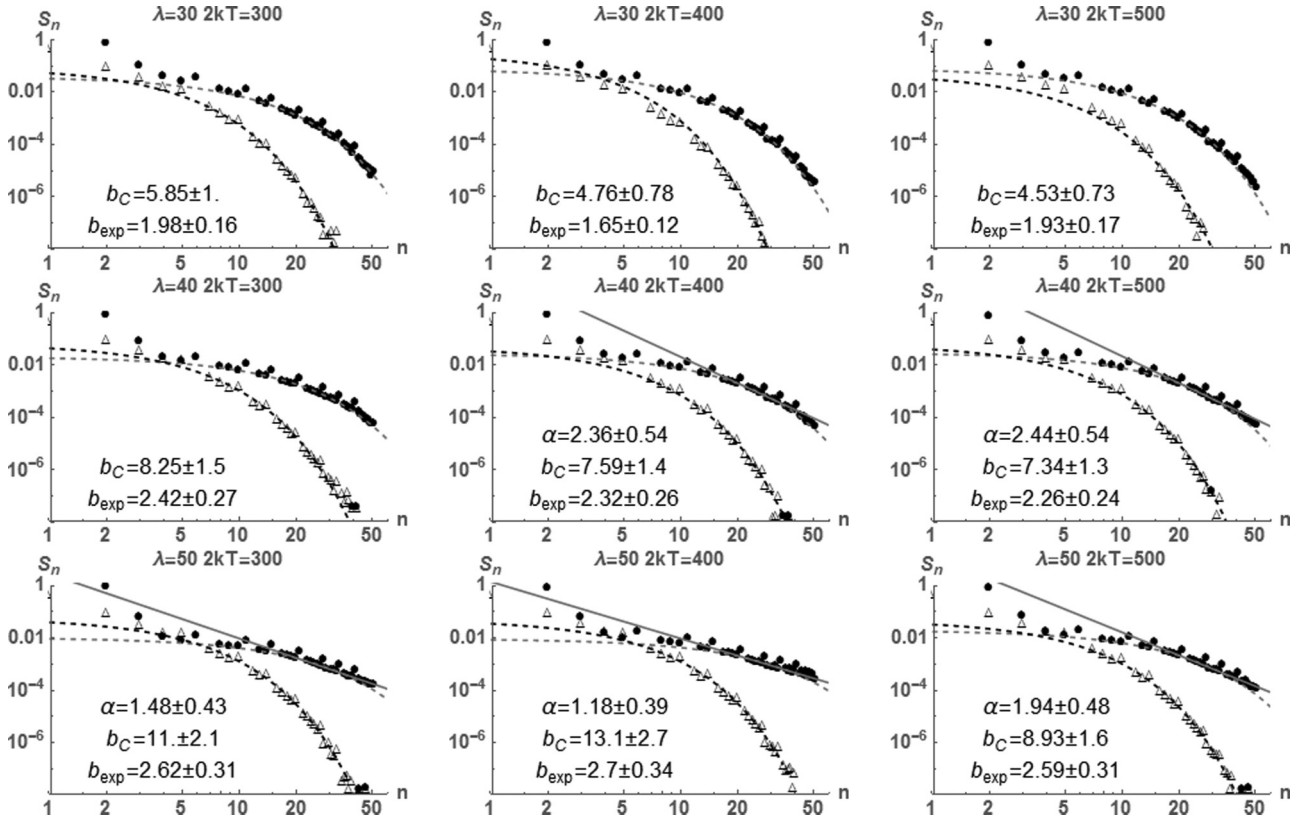

FIG. 2. The probability distribution S_n of finding the n-segment-long linearized fragment in a chain driven by the spatially correlated noise. Each plot represents the results for noise amplitude $2kT$ and correlation length λ. Triangles: exponential noise correlation function $\langle \boldsymbol{\xi}(\mathbf{r})\boldsymbol{\xi}(\mathbf{r}+\Delta\mathbf{r})\rangle \propto \exp(-|\Delta\mathbf{r}|/\lambda)$; dots: Cauchy noise correlation function $\langle \boldsymbol{\xi}(\mathbf{r})\boldsymbol{\xi}(\mathbf{r}+\Delta\mathbf{r})\rangle \propto 1/[1+(|\Delta\mathbf{r}|/\lambda)^2]$. The tail behavior ($n \geqslant 17$) has been fitted with exponential decay model $S_n = ce^{-n/b_i}$ (dashed lines) with b_i given on the plot. For $\lambda \geqslant 40$ the data has been also fitted with power law $S_n = cn^{-(\alpha+1)}$ for $n \geqslant 17$, indicating the power-law asymptotic behavior.

where we made use of α stability. For $\alpha = 2$ this formula comes down to the well known result for Gaussian chain [1]:

$$G(|\mathbf{r}_i - \mathbf{r}_j|) = \left(\frac{2\pi|i-j|b^2}{D}\right)^{-D/2} \exp\left(-\frac{D(\mathbf{r}_i-\mathbf{r}_j)^2}{2|i-j|b^2}\right). \tag{10}$$

It is also possible to calculate $\alpha = 1$ case explicitly:

$$P_{\alpha=1,D=3}(|\mathbf{r}_i - \mathbf{r}_j|) = \frac{16\pi|i-j|}{3}\frac{1}{\left(\frac{4|i-j|^2}{9}+r^2\right)^2}. \tag{11}$$

In particular, taking as i and j the first and the last segment respectively, we obtain the end-to-end distance distribution.

A classical problem in polymer physics is to predict the scaling behavior of radius of gyration R_g with the growing N. In order to do so, we will calculate R_g using a method mentioned in Ref. [13], namely $R_g = \langle r^\alpha\rangle^{1/\alpha}$, where $\langle . \rangle$ denotes the average:

$$\begin{aligned} R_g &= \left[\frac{1}{(2\pi)^D}\int d\mathbf{r} r^\alpha \int d\mathbf{k} \exp\left(i\mathbf{k}\cdot\mathbf{r} - \frac{2N}{D}b^\alpha k^\alpha\right)\right]^{1/\alpha} \\ &= b\left(\frac{2N}{D}\right)^{1/\alpha} \\ &\quad \times \left(\frac{1}{(2\pi)^D}\int d\mathbf{r}' r'^\alpha \int d\mathbf{k}' \exp(i\mathbf{k}'\cdot\mathbf{r}' - k'^\alpha)\right)^{1/\alpha}. \end{aligned} \tag{12}$$

This result is obtained via the change of variables $\mathbf{k}' = b(2N/D)^{1/\alpha}\mathbf{k}$ and $\mathbf{r}' = b^{-1}(2N/D)^{-1/\alpha}\mathbf{r}$, which completely factors the dependence on b and N out of the integral. Therefore, the scaling reads $R_g \propto bN^{1/\alpha}$.

While this scaling seems reasonable for $\alpha \geqslant 1$, it becomes questionable for $0 < \alpha < 1$, for which the scaling exponent of N becomes greater than 1. On the one hand, the examples from Sec. II use $\alpha \geqslant 1$ almost exclusively. In particular, Moon and Nakanishi in Ref. [13] introduce their more complicated Levy walk model to avoid $\alpha < 1$ problem and, in their approach, the scaling exponent of N is always lower than 1. On the other hand, Bouchaud and Daoud in Ref. [25] systematically discuss every possible value of α, pointing out that for $\alpha < 1$ the Flory correction from the self-avoiding nodes becomes irrelevant. In

conclusion, while $\alpha < 1$ seems physically unlikely, with so little literature on the subject it cannot be rejected at this point.

Finally, with $P(|\mathbf{r}_{i+1} - \mathbf{r}_i|)$ at our disposal, we can calculate the distribution of nodes around the mass center of the chain. This derivation is highly technical, so we include it in Appendix and here we discuss the final result only. In the limit of huge number of nodes N, the sought distribution reads:

$$P_{\mathrm{CM}}(|\mathbf{r}-\mathbf{R}|) = \frac{1}{(2\pi)^D}\int_0^1 dq \int d\mathbf{k}\exp\left[i\mathbf{k}\cdot(\mathbf{r}-\mathbf{R}) - \frac{2Nb^\alpha k^\alpha}{D(\alpha+1)}\left((1-q)^{\alpha+1}+q^{\alpha+1}\right)\right], \quad (13)$$

where $\mathbf{R}$ is the mass center. While this expression is exact, the integral with respect to q makes it unwieldy. We can simplify it by resorting to the integral mean value theorem. Namely, there exists such $q_0 \in [0,1]$, that:

$$P_{\mathrm{CM}}(|\mathbf{r}-\mathbf{R}|) = \frac{1}{(2\pi)^D}\int d\mathbf{k}\exp\left[i\mathbf{k}_0\cdot(\mathbf{r}-\mathbf{R}) - \frac{2Nb^\alpha k^\alpha}{D(\alpha+1)}\left((1-q_0)^{\alpha+1}+q_0^{\alpha+1}\right)\right]. \quad (14)$$

On the other hand, since the integrand of (13) is a peak function of q with maximum at $q = 1/2$, this value contributes the most to the integral. For this reason, we will approximate (14) by imposing $q_0 = 1/2$. This results in the characteristic function of $P_{\mathrm{CM}}(|\mathbf{r}-\mathbf{R}|)$ in a form $\exp(-c(\alpha)k^\alpha)$, where:

$$c(\alpha) = \frac{2N}{D(\alpha+1)}\left(\frac{b}{2}\right)^\alpha. \quad (15)$$

IV. COARSE-GRAINED INTERACTION BETWEEN TWO NON-GAUSSIAN POLYMERS

Having established $P_{\mathrm{CM}}(|\mathbf{r}-\mathbf{R}|)$ for a single chain, we can calculate the coarse-grained interaction between two chains in terms of the distance between their mass centers. From now on, the lower index numerates the type of particle, so $P_{\mathrm{CM},i}(|\mathbf{r}-\mathbf{R}_i|)$ describes an ith type of chain characterized by N_i segments, constant b_i and exponent α_i. We can follow the reasoning of Flory and Krigbaum [3] and assume that the systems suffers an energetic penalty ϵ_{ij} if a segment belonging to one chain invades a small volume in the vicinity of a segment belonging to the other chain. For a single site $\mathbf{r}$, the probability of such event is proportional to $P_{\mathrm{CM},i}(|\mathbf{r}-\mathbf{R}_i|)P_{\mathrm{CM},j}(|\mathbf{r}-\mathbf{R}_j|)d\mathbf{r}$. Therefore, the entire interaction reads:

$$\begin{aligned} V_{ij}(|\mathbf{R}_i-\mathbf{R}_j|) &= \epsilon_{ij}\tilde{c}_{ij}\int d\mathbf{r}P_{\mathrm{CM},i}(|\mathbf{r}-\mathbf{R}_i|)P_{\mathrm{CM},j}(|\mathbf{r}-\mathbf{R}_j|) \\ &= \frac{\epsilon_{ij}\tilde{c}_{ij}}{(2\pi)^D}\int d\mathbf{k}\exp[i\mathbf{k}\cdot(\mathbf{R}_i-\mathbf{R}_j) \\ &\quad - c_i(\alpha_i)k^{\alpha_i} - c_j(\alpha_j)k^{\alpha_j}]. \end{aligned} \quad (16)$$

Assuming that ϵ_{ij} has a dimension of energy, it is necessary to introduce an additional constant $\tilde{c}_{ij}$, which has a dimension of volume. We can deduce this constant from the case of $\alpha_i = \alpha_j = 2$, for which we obtain the following universal Gaussian potential [8] and its Fourier transform:

$$V(r) = \epsilon\exp\left(-\frac{r^2}{4c}\right) \qquad \mathcal{V}(k) = \epsilon\,(4\pi c)^{D/2}\,e^{-ck^2}. \quad (17)$$

When ϵ is independent from N, this potential is perceived as an accurate and reliable model for interaction of identical chains [8,9]. Comparing (17) to (16), one can see that $c = c_i(2) + c_j(2)$ and hence $\tilde{c}_{ij} = (4\pi c)^{D/2}$. This can be generalized for $\alpha_i = \alpha_j = \alpha$ by:

$$\tilde{c}_{ij} = \{4\pi[c_i(\alpha) + c_j(\alpha)]\}^{D/\alpha}. \quad (18)$$

For the case of $\alpha_i \neq \alpha_j$ the constant $\tilde{c}_{ij}$ cannot be uniquely deduced from the dimensional analysis, thus we will restrict our further considerations to the potentials with common α.

V. EFFECTIVE INTERACTIONS AND MIXTURE STABILITY

Once V_{ij} has been found, we can analyze the interactions in binary mixtures. The system is described by three microscopic potentials in the form (16), where V_{11} and V_{22} are the internal interactions of each species and V_{12} is the cross-species interaction. When the behavior of one species in a mixture is considered, the presence of the other species modifies the microscopic interaction [7,8]. The additional potential, known as the effective interaction, is of entropic origin [7,8] and it is a key factor in controlling mixture stability and demixing. The prediction of effective interactions from arbitrary microscopic potentials is usually a challenging numerical task, but in our previous work [12] we have proposed a simple analytical method, suitable for soft interactions. According to Ref. [12], the effective interaction can be estimated by:

$$U_{\mathrm{eff}}(\Delta R) = -\frac{1}{(2\pi)^D}\int_{\tilde{\Omega}} d\mathbf{k}e^{i\mathbf{k}\cdot\Delta\mathbf{R}}\frac{|\mathcal{V}_{12}(k)|^2}{\mathcal{V}_{22}(k)}, \quad (19)$$

where $\mathcal{V}_{ij}(k) = \int d\mathbf{r}\exp(i\mathbf{k}\cdot\mathbf{r})V_{ij}(r)$ is a Fourier transform of relevant $V_{ij}(r)$ and $\tilde{\Omega}$ is the volume in the reciprocal space. Substituting (16) with relevant constants given by (18) into the expression for effective interactions, one obtains:

$$U_{\mathrm{eff}}(\Delta R) = -\frac{1}{(2\pi)^D}\frac{\epsilon_{12}^2}{\epsilon_{22}}\frac{(4\pi)^{D/\alpha}[c_1(\alpha)+c_2(\alpha)]^{2D/\alpha}}{[2c_2(\alpha)]^{D/\alpha}} \times \int_{\tilde{\Omega}} d\mathbf{k}e^{i\mathbf{k}\cdot\Delta\mathbf{R}-2c_1(\alpha)k^\alpha}. \quad (20)$$

The total interaction for the first species in the mixture reads:

$$U_{\mathrm{tot}}(\Delta R) = V_{11}(\Delta R) + U_{\mathrm{eff}}(\Delta R) \quad (21)$$

or explicitly:

$$\begin{aligned} U_{\mathrm{tot}}(r) &= \left(\epsilon_{11}\,[8\pi c_1(\alpha)]^{D/\alpha} - \frac{\epsilon_{12}^2}{\epsilon_{22}}\frac{(4\pi)^{D/\alpha}[c_1(\alpha)+c_2(\alpha)]^{2D/\alpha}}{[2c_2(\alpha)]^{D/\alpha}}\right) \\ &\quad \times\frac{1}{(2\pi)^D}\int_{\tilde{\Omega}} d\mathbf{k}e^{i\mathbf{k}\cdot\Delta\mathbf{R}-2c_1(\alpha)k^\alpha}. \end{aligned} \quad (22)$$

One can see that $U_{\rm tot}(\Delta R)$ and $V_{11}(\Delta R)$ have the same shape, up to the scaling factor S:

$$S = \epsilon_{11}\,[8\pi c_1(\alpha)]^{D/\alpha} - \frac{\epsilon_{12}^2}{\epsilon_{22}}\frac{(4\pi)^{D/\alpha}[c_1(\alpha)+c_2(\alpha)]^{2D/\alpha}}{[2c_2(\alpha)]^{D/\alpha}}. \tag{23}$$

S has a complicated form and it can take both the negative and positive values, depending on the parameters. The change in the sign of the total interaction indicates a remarkable change in the behavior of the system. Namely, for $S > 0$ the total interaction between the particles of the first species is purely repulsive, which means that these particles will disperse in the volume. Conversely, for $S < 0$, the first species of particles interacts via attractive potential, which results in the clustering of these particles and demixing in the system. Equating S to 0, the condition for demixing reads:

$$\frac{\epsilon_{11}\epsilon_{22}}{\epsilon_{21}^2} < \left(\frac{[c_1(\alpha)+c_2(\alpha)]^2}{4c_1(\alpha)c_2(\alpha)}\right)^{D/\alpha}. \tag{24}$$

Let us now analyze the condition (24) and introduce a common energy scale:

$$\tilde{\epsilon} = \frac{\epsilon_{12}}{\sqrt{\epsilon_{11}\epsilon_{22}}} \tag{25}$$

and:

$$g = \left(\frac{c_1(\alpha)}{c_2(\alpha)}\right)^{1/\alpha} = \frac{b_1}{b_2}\left(\frac{N_1}{N_2}\right)^{1/\alpha} \tag{26}$$

for which condition (24) can be reduced to:

$$\tilde{\epsilon} > \left(\frac{4g^\alpha}{(1+g^\alpha)^2}\right)^{D/(2\alpha)}. \tag{27}$$

Recalling the equation (12) for the radius of gyration R_g, one can see that for the chains characterized by the distributions sharing the same α, the parameter g becomes the ratio of R_g:

$$g = \frac{R_{g,1}}{R_{g,2}}. \tag{28}$$

For $\alpha = 2$ and $D = 3$ the condition (24) becomes exactly the spinodal decomposition condition for Gaussian particles, as given in Ref. [5] and [6], namely:

$$\tilde{\epsilon} > \left(\frac{2g}{1+g^2}\right)^{3/2}. \tag{29}$$

Therefore, the condition (27) is a direct generalization of the spinodal decomposition to the systems of particles described with α-stable distributions.

The condition (27) is plotted in Fig. 3. For every pair of g and α its value varies from 0 to 1. In the entire range of α, the region of mixing (below the surface) preserves the features of the Gaussian case, namely it falls rapidly to 0 for $g \ll 1$, reaches the single maximum at $g = 1$, and asymptotically decreases to 0 for $g \gg 1$. However, as α decreases to 0 the mixing region for $g \gg 1$ becomes wider, asymptotically reaching the region defined by $\tilde{\epsilon} > 1$. This means that the gyration radius ratio g becomes less and less relevant for the mixing of chains characterized by very wide distributions. The changes in the mixing region shape are much more pronounced for $\alpha < 1$.

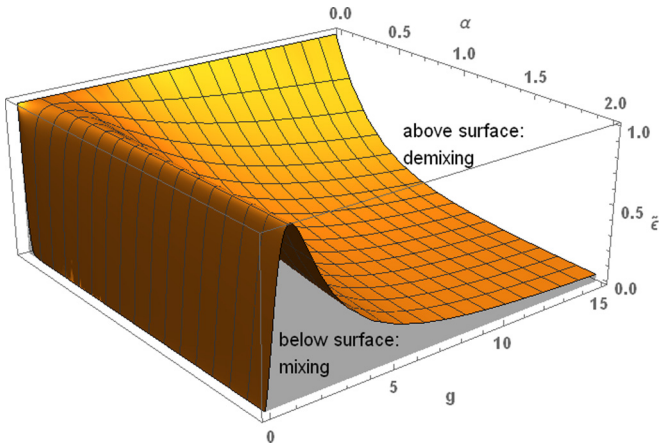

FIG. 3. (Color online) The spinodal decomposition condition (27) for the binary systems of particles described with the α-stable statistics as a function of gyration radii ratio $g = R_{g,1}/R_{g,2}$ and the distribution exponent α for $D = 3$ dimensional system. $\tilde{\epsilon} = \epsilon_{12}/\sqrt{\epsilon_{11}\epsilon_{22}}$ is the common energy scale. In the region above the plotted surface the binary system undergoes demixing due to the prevalence of the attractive effective interactions, in the region below the surface the effective interaction is repulsive and the system is homogeneous.

VI. DISCUSSION

It is known that the spinodal decomposition condition for Gaussian particles leads to the predictions on mixture separation, which are qualitatively and quantitatively comparable to the more advanced methods [6]. Thus, a similar efficiency can be expected from (27), at least for α mildly deviating from 2. However, some possible issues should be mentioned.

The fact that the total interaction (21) can become entirely negative is unrealistic. This evident problem is mitigated by the fact that the energy density of a pair interaction behaves as $U_{\rm tot}(r)r^{D-1}dr$. Therefore, r^{D-1} factor suppresses the lack of repulsive core at short distances and amplifies the influence of the attractive tail. The unrealistic shape of $U_{\rm tot}$ is also a consequence of the way the potential $V_{ij}(r)$ given by (16) is constructed. This potential is mean field in its nature and its width is governed by the constant $c_i(\alpha) + c_j(\alpha)$. In the context of Gaussian particles, while the dominant shape of the interaction between two separate chains is agreed to be Gaussian [9,33], there is an open problem of whether there are additional components [33] or how the width of such Gaussian is related to the gyration radii of the component chains [5]. A similar problem is relevant in our case and the choice of the width constant different from $c_i(\alpha) + c_j(\alpha)$ might result in a more realistic shape of $U_{\rm tot}$

VII. PHASE SEPARATION IN THE ADSORPTION OF GAUSSIAN PARTICLES TO THE SURFACE

The result (27) is particularly interesting in the context of the already mentioned work of Bouchaud and Daoud [25], where the gyration radius parallel to the surface is calculated for an adsorbed polymer. As mentioned in Sec. II, the characteristic exponent for the distribution on the surface reads $\alpha_{ss} = 2$ in the strong adsorption limit and $\alpha_{ws} = 1$ in the weak

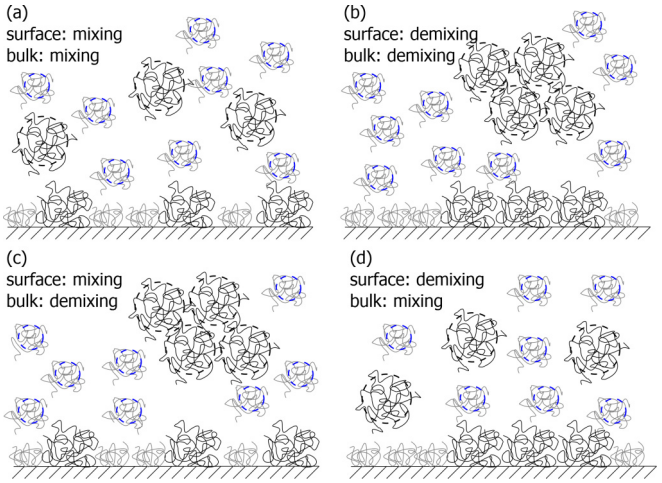

FIG. 4. (Color online) Schematic representation of four mixing and demixing scenarios in the binary system consisting of a solution and an adsorbing surface. In the bulk polymers follow the Gaussian statistics ($\alpha_b = 2$, $D_b = 3$). On the surface ($D_s = 2$) polymers are described either by $\alpha_{ss} = 2$ in the strong adsorption limit or $\alpha_{ws} = 1$ for the weak adsorption.

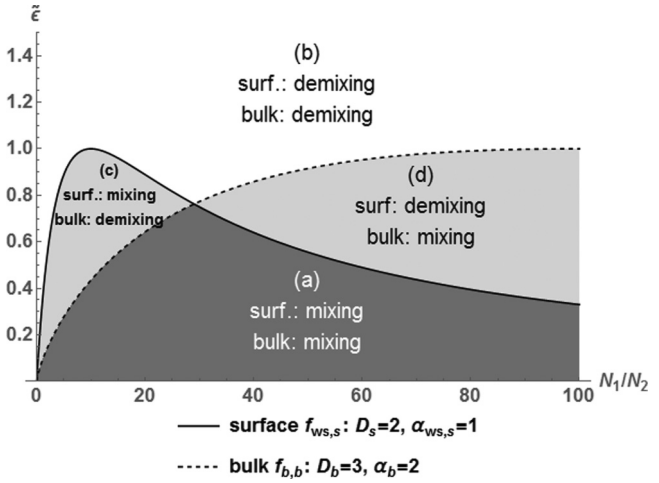

FIG. 5. The exemplary comparison of the phase separation conditions on the surface in the weak adsorption limit ($f_{ws,s}$, solid line) and in the bulk ($f_{b,b}$, dashed line) for the binary system of Gaussian polymers characterized by the persistence length ratio $b_1/b_2 = 0.1$. $f_{ws,s}$ and $f_{b,b}$ are defined by (30). $f_{ws,s}$ and $f_{b,b}$ divide the plot into four regions: (a) simultaneous mixing on the surface and in the bulk, (b) simultaneous demixing on the surface and in the bulk, (c) mixing on the surface, demixing in the bulk, (d) demixing on the surface, mixing in the bulk.

adsorption limit [25]. Considering the adsorption from the binary mixture, (27) provides the condition for homogeneous versus inhomogeneous adsorption, i.e., the ratio of gyration radii parallel to the surface ($R_{g,||}$) decides whether both species cover the surface in a homogeneous manner or they separate into the islands consisting of the particles of the same type. On the other hand (27) allows us to compare for which parameters the separation on the surface and in the bulk coappear.

Let us consider a simple binary system in which the behavior of chains in the bulk ($D_b = 3$, $\alpha_b = 2$) is Gaussian, but on the surface it is characterized by $D_s = 2$ and α_{ss} or α_{ws}. The types of particles differ by the number of monomers N_i and their persistence length b_i. The condition (27) reads:

$$\tilde{\epsilon} > \left(\frac{4 \left(\frac{b_1}{b_2}\right)^{\alpha_x} \frac{N_1}{N_2}}{\left[1 + \left(\frac{b_1}{b_2}\right)^{\alpha_x} \frac{N_1}{N_2}\right]^2} \right)^{\frac{D_y}{2\alpha_x}} = f_{x,y}. \qquad (30)$$

In the strong adsorption limit it is always true that $f_{ss,s} \geqslant f_{b,b}$ for any b_1/b_2 and N_1/N_2. Therefore, assuming that in this system $\tilde{\epsilon}$ is the same on the surface and in the bulk, three scenarios of mixing or demixing are allowed. First, for (a) [Fig. 4(a)] $f_{ss,s} \geqslant f_{b,b} \geqslant \tilde{\epsilon}$ the solution in the bulk is homogeneous and so is the coverage of the surface. Conversely, for (b) [Fig. 4(b)] $\tilde{\epsilon} \geqslant f_{ss,s} \geqslant f_{b,b}$ the separation is simultaneous on the surface and in the bulk. Finally, for (c) [Fig. 4(c)] $f_{ss,s} \geqslant \tilde{\epsilon} \geqslant f_{b,b}$ demixing in the bulk occurs, but the surface coverage is still homogeneous. The schematic representation of scenarios (a)–(c) is shown in Fig. 4.

In the weak adsorption limit ($\alpha_{ws} = 1$), the situation is more complicated because both $f_{ws,s} \geqslant f_{b,b}$ and $f_{ws,s} \leqslant f_{b,b}$ are possible, depending on b_1/b_2 and N_1/N_2. Replacing $f_{ss,s}$ by $f_{ws,s}$ in the inequalities from the previous paragraph one obtains the conditions for separation scenarios (a)–(c) in the weak adsorption limit. However, there exists the additional region in which it is possible that (d) [Fig. 4(d)] $f_{b,b} \geqslant \tilde{\epsilon} \geqslant f_{ws,s}$. In this region the separation on the surface occurs, while the solution in the bulk is still homogeneous (see Fig. 4). In Fig. 5 the exemplary phase separation diagram for the weak adsorption limit and $b_1/b_2 = 0.1$ is presented, which contains all of the phase separation scenarios (a)–(d). Figure 6 shows the difference $f_{ws,s} - f_{b,b}$, which indicates where scenarios (c) and (d) are allowed. In particular, for $b_1/b_2 \to 0$ and $b_1/b_2 \gg 1$ the scenario (d) becomes almost inaccessible, while it is allowed in the vicinity of $b_1/b_2 \simeq 1$.

These considerations show that the behavior of a mixture can be designed by the choice of b_1/b_2 (which is dependent on the chemical composition) and N_1/N_2. However, our predictions can be affected by a few additional effects. In general, there are two main factors that determine the behavior of the system as a whole. On the one hand, the system tends to minimize its energy, so the details of adsorption mechanism (e.g., binding energy, a preference for a certain type of particles, adsorption rate, etc.) are important. Since our model is valid for thermodynamic equilibrium, the surface binding should not be significantly stronger than other interactions, to allow equilibration. On the other hand, the system globally maximizes its entropy, which includes the on-surface and in-the-bulk contributions. However, there is also the bulk-surface component, i.e., the bigger particles can decrease their excluded volume in the vicinity of a wall, hence they experience the entropy-driven affinity to the flat surface [7,34]. This effect is not included in our model. One would generally expect the increased concentration of bigger particles in the near-surface region and a reduced availability of smaller particles. Indeed, for the hard-sphere mixtures this effect depends on the concentration of smaller particles and it precedes the in-bulk clustering [34], which can be also expected for polymers. It is not clear, however, whether this

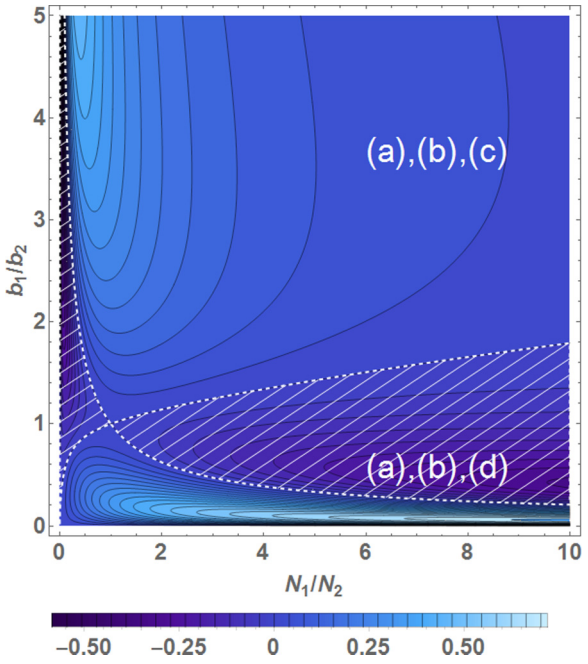

FIG. 6. (Color online) The density plot of the difference $f_{ws,s} - f_{b,b}$ as a function of persistence length ratio b_1/b_2 and the ratio of monomer numbers N_1/N_2. $f_{ws,s} - f_{b,b}$ indicates which surface/bulk demixing scenarios are allowed (see Sec. VII and Fig. 5 for explanation). White meshed region: $f_{ws,s} - f_{b,b} < 0$ indicates scenario (d) allowed (demixing on the surface, mixing in the bulk), complement region: $f_{ws,s-} f_{b,b} > 0$ scenario (c) allowed (mixing on the surface, demixing in the bulk).

effect can be strong enough to result in the complete coating of the surface with bigger particles.

In conclusion, the full theory should also include both the detailed adsorption mechanism and the surface affinity. However, our model is potentially valid in the semidilute regime for adsorption strength comparable to entropic interactions and in the systems in which the surface effects are a significant contribution to the entropy of the entire system.

VIII. SUMMARY

In summary, in this paper we have presented the generalization of the results known from the Gaussian chain theory to the particles described with the α-stable distributions. As expected, it is possible to obtain a similar hierarchy of analytical results ranging from end-to-end distribution up to the effective interactions in binary mixtures. Typically for α-stable distributions, we obtained the closed-form formulas in the Fourier space. Our theory also allows us to generalize the spinodal decomposition condition from Gaussian particles to the α-stable particles. This can be readily applied to the problem of mixing or demixing of adsorbed polymers, as we also show. Our results might be further utilized in the context of Levy flights applications reviewed in Sec. II.

APPENDIX: DISTRIBUTION OF SEGMENTS AROUND THE CENTER OF MASS

In this Appendix we derive the distribution of segments around the mass center of a chain. Let us consider an N-segments-long chain, described by the nearest-neighbor probability given by (8). The position of the mass center reads:

$$\mathbf{R} = \frac{1}{N}\sum_{i=1}^{N}\mathbf{r}_i. \tag{A1}$$

The probability that each segment occupies its position $\mathbf{r}_i$ under condition that the mass center is positioned at $\mathbf{R}$ reads:

$$P(\mathbf{r}_1,\ldots,\mathbf{r}_N|\mathbf{R}) = \prod_{i=1}^{N-1} P(|\mathbf{r}_{i+1}-\mathbf{r}_i|)\delta\left(\mathbf{R} - \frac{1}{N}\sum_{i=1}^{N}\mathbf{r}_i\right). \tag{A2}$$

From this expression we can calculate the probability of finding jth segment at some position relative to the mass center:

$$P(|\mathbf{r}_j - \mathbf{R}|) = \int d\mathbf{r}_1 \ldots \int d\mathbf{r}_{j-1} \int d\mathbf{r}_{j+1} \ldots \int d\mathbf{r}_N \times \prod_{i=1}^{N-1} P(|\mathbf{r}_{i+1}-\mathbf{r}_i|)\delta\left(\mathbf{R} - \frac{1}{N}\sum_{i=1}^{N}\mathbf{r}_i\right). \tag{A3}$$

The integrals in the above expression can be done particularly easily, if we switch to relative variables:

$$\begin{aligned} \Delta\mathbf{r}_{i-j} &= \mathbf{r}_i - \mathbf{r}_{i-1} \quad \text{for} \quad i > j \\ \Delta\mathbf{r}_{i-j} &= \mathbf{r}_{i-1} - \mathbf{r}_i \quad \text{for} \quad i < j, \end{aligned} \tag{A4}$$

which allows us to express $\mathbf{r}_i$ as:

$$\begin{aligned} \mathbf{r}_i &= \mathbf{r}_j + \sum_{n=1}^{N-i}\Delta\mathbf{r}_{+n} \quad \text{for} \quad N \geqslant i > j \\ \mathbf{r}_i &= \mathbf{r}_j + \sum_{n=1}^{j-i}\Delta\mathbf{r}_{-n} \quad \text{for} \quad 1 \leqslant i < j. \end{aligned} \tag{A5}$$

In these coordinates the position of mass center reads:

$$\frac{1}{N}\sum_{i=1}^{N}\mathbf{r}_i = \mathbf{r}_j + \sum_{n=1}^{N-j}\frac{N-j-n+1}{N}\Delta\mathbf{r}_{+n} + \sum_{n=1}^{j-1}\frac{j-n}{N}\Delta\mathbf{r}_{-n}. \tag{A6}$$

The change of variables (A4) is linear and its Jacobian is equal to 1, so applying the new coordinates to (A3), we obtain:

$$P(|\mathbf{r}_j - \mathbf{R}|) = \prod_{\substack{n=-j \\ n\neq 0}}^{N-j}\int d\Delta\mathbf{r}_n P(\Delta r_n) \times\delta\left(\mathbf{R} - \mathbf{r}_j + \sum_{n=1}^{N-j}\frac{N-j-n+1}{N}\Delta\mathbf{r}_{+n} + \sum_{n=1}^{j-1}\frac{j-n}{N}\Delta\mathbf{r}_{-n}\right). \tag{A7}$$

The following step is to express $P(\Delta r_n)$ in (A7) in terms of its characteristic function (8):

$$P(|\mathbf{r}_j-\mathbf{R}|)=\frac{1}{(2\pi)^{ND}}\prod_{\substack{n=-j\\ n\neq 0}}^{N-j}\int d\Delta\mathbf{r}_n\int d\mathbf{k}_n e^{i\mathbf{k}_n\cdot\Delta\mathbf{r}_n}\phi(k_n)\times\int d\mathbf{k}_0\exp\left(i\mathbf{k}_0\cdot(\mathbf{R}-\mathbf{r}_j)+i\sum_{n=1}^{N-j}\frac{N-j-n+1}{N}\mathbf{k}_0\cdot\Delta\mathbf{r}_{+n}+i\sum_{n=1}^{j-1}\frac{j-n}{N}\mathbf{k}_0\cdot\Delta\mathbf{r}_{-n}\right). \tag{A8}$$

Further, we integrate out every component of $\Delta\mathbf{r}_{\pm n}$, which introduces multiple Dirac-δ functions:

$$\begin{aligned}P(|\mathbf{r}_j-\mathbf{R}|)&=\frac{1}{(2\pi)^D}\\&=\int d\mathbf{k}_0\left[\prod_{n=1}^{N-j}\int d\mathbf{k}_{+n}\phi(k_{+n})\times\delta\left(\mathbf{k}_{+n}-\frac{N-j-n+1}{N}\mathbf{k}_0\right)\right]\\&\quad\times\left[\prod_{n=1}^{j-1}\int d\mathbf{k}_{-n}\phi(k_{-n})\delta\left(\mathbf{k}_{-n}-\frac{j-n}{N}\mathbf{k}_0\right)\right]e^{i\mathbf{k}_0\cdot(\mathbf{R}-\mathbf{r}_j)}\\&=\frac{1}{(2\pi)^D}\int d\mathbf{k}_0\left[\prod_{n=1}^{N-j}\phi\left(\frac{N-j-n+1}{N}k_0\right)\right]\\&\quad\times\left[\prod_{n=1}^{j-1}\phi\left(\frac{j-n}{N}k_0\right)\right]e^{i\mathbf{k}_0\cdot(\mathbf{R}-\mathbf{r}_j)}.\end{aligned} \tag{A9}$$

At this point we apply the explicit form of $\phi(k)$, so the final expression for $P(|\mathbf{r}_j-\mathbf{R}|)$ reads:

$$P(|\mathbf{r}_j-\mathbf{R}|)=\frac{1}{(2\pi)^D}\int d\mathbf{k}_0\exp\left\{i\mathbf{k}_0\cdot(\mathbf{R}-\mathbf{r}_j)-\frac{2b^\alpha}{D}\left[\sum_{n=1}^{N-j}\left(\frac{N-j-n+1}{N}\right)^\alpha+\sum_{n=1}^{j-1}\left(\frac{j-n}{N}\right)^\alpha\right]k_0^\alpha\right\}. \tag{A10}$$

Expression (A10) gives the probability of finding jth segment in the vicinity of mass center, so the probability of finding any segment reads:

$$P_{\mathrm{CM}}(|\mathbf{r}-\mathbf{R}|)=\frac{1}{N}\sum_{j=1}^{N}P(|\mathbf{r}_j-\mathbf{R}|), \tag{A11}$$

where the factor $1/N$ provides normalization. Let us assume now that N is a large number, so both $n/N=q$ and $j/N=q'$ can be treated as continuous variables, hence we can simplify:

$$\sum_{n=1}^{N-j}\left(\frac{N-j-n+1}{N}\right)^\alpha\to N\int_0^{1-q'}dq(1-q'-q)^\alpha=\frac{N}{\alpha+1}(1-q')^{\alpha+1} \tag{A12}$$

$$\sum_{n=1}^{j-1}\left(\frac{j-n}{N}\right)^\alpha\to N\int_0^{q'}dq(q'-q)^\alpha=\frac{N}{\alpha+1}q'^{\alpha+1}. \tag{A13}$$

The final expression for the distribution of any segment around the mass center reads:

$$P_{\mathrm{CM}}(|\mathbf{r}-\mathbf{R}|)=\frac{1}{(2\pi)^D}\int_0^1 dq'\int d\mathbf{k}_0\exp\left[i\mathbf{k}_0\cdot(\mathbf{r}-\mathbf{R})-\frac{2Nb^\alpha k_0^\alpha}{D(\alpha+1)}((1-q')^{\alpha+1}+q'^{\alpha+1})\right]. \tag{A14}$$

[1] I. Teraoka, *Polymer solutions: an Introduction to Physical Properties* (Wiley, New York, 2002).
[2] P. Debye and F. Bueche, J. Chem. Phys. **20**, 1337 (1952).
[3] P. J. Flory and W. R. Krigbaum, J. Chem. Phys. **18**, 1086 (1950).
[4] G. Samorodnitsky and M. S. Taqqu, *Stable Non-Gaussian Random Processes: Stochastic Models with Infinite Variance* (Chapman and Hall, New York, 1994).
[5] A. A. Louis, P. G. Bolhuis, and J. P. Hansen, Phys. Rev. E **62**, 7961 (2000).
[6] R. Finken, J. P. Hansen, and A. A. Louis, J. Stat. Phys. **110**, 1015 (2003).
[7] H. N. W. Lekkerkerker and R. Tuinier, *Colloids and the Depletion Interaction* (Springer, London, 2011).
[8] C. N. Likos, Phys. Rep. **348**, 267 (2001).
[9] P. G. Bolhuis, A. A. Louis, J. P. Hansen, and E. J. Meijer, J. Chem. Phys. **114**, 4296 (2001).
[10] G. Yatsenko, E. J. Sambriski, M. A. Nemirovskaya, and M. Guenza, Phys. Rev. Lett. **93**, 257803 (2004).
[11] J. McCarty, I. Y. Lyubimov, and M. G. Guenza, Macromolecules **43**, 3964 (2010).
[12] M. Majka and P. F. Góra, Phys. Rev. E **90**, 032303 (2014).
[13] J. Moon and H. Nakanishi, Phys. Rev. A **42**, 3221 (1990).
[14] M. F. Shlesinger, B. J. West, and J. Klafter, Phys. Rev. Lett. **58**, 1100 (1987).
[15] F. Valle, M. Favre, P. De Los Rios, A. Rosa, and G. Dietler, Phys. Rev. Lett. **95**, 158105 (2005).
[16] T. E. Fisher, A. F. Oberhauser, M. Carrion-Vazquez, P. E. Marszalek, and J. M. Fernandez, Trends Biochem. Sci. **24**, 379 (1999).

[17] G. W. Daughdrill, G. J. Pielak, V. N. Uversky, M. S. Cortese, and A. K. Dunker, *Natively Disordered Proteins, in Protein Folding Handbook*, edited by J. Buchner and T. Kiefhaber (Wiley-VCH Verlag GmbH, Weinheim, 2005).
[18] V. N. Uversky and A. K. Dunker, BBA-Proteins Proteom **1804**, 1231 (2010).
[19] N. C. Fitzkee and G. D. Rose, Proc. Natl. Acad. Sci. USA **101**, 12497 (2004).
[20] J. Elf, G. W. Li, and X. S. Xie, Science **316**, 1191 (2007).
[21] L. Mirny, M. Slutsky, Z. Wunderlich, A. Tafvizi, J. Leith, and A. Kosmrlj, J. Phys. A: Math. Theor. **42**, 434013 (2009).
[22] M. A. Lomholt, T. Ambjörnsson, and R. Metzler, Phys. Rev. Lett. **95**, 260603 (2005).
[23] P. G. de Gennes, J. Phys. France **37**, 1445 (1976).
[24] P. G. de Gennes and P. Pincus, J. Physique Lett. **44**, 241 (1983).
[25] E. Bouchaud and M. Daoud, J. Phys. A: Math. Gen. **20**, 1463 (1987).
[26] C. Donati, S. C. Glotzer, P. H. Poole, W. Kob, and S. J. Plimpton, Phys. Rev. E **60**, 3107 (1999).
[27] B. Doliwa and A. Heuer, Phys. Rev. E **61**, 6898 (2000).
[28] A. C. Mitus, A. Z. Patashinski, A. Patrykiejew, and S. Sokolowski, Phys. Rev. B **66**, 184202 (2002).
[29] J. J. Binney *et al.*, *The Theory of Critical Phenomena* (Oxford University Press, Oxford, 1992).
[30] M. Majka and P. F. Góra, Phys. Rev. E **86**, 051122 (2012).
[31] M. Majka and P. F. Góra, Acta Phys. Pol. B **44**, 1099 (2013).
[32] K. Szczepaniec and B. Dybiec, Phys. Rev. E **90**, 032128 (2014).
[33] J. Dautenhahn and C. K. Hall, Macromolecules **27**, 5399 (1994).
[34] A. G. Yodh, K. Lin, J. C. Crocker, A. D. Dinsmore, R. Verma, and P. D. Kaplan, Phil. Trans. R. Soc. Lond. A **359**, 921 (2001).